The Astrophysical Journal, 768:29 (6pp), 2013 May 1 doi:10.1088/0004-637X/768/1/29

MASSIVE BLACK HOLES IN CENTRAL CLUSTER GALAXIES

Marta Volonteri[1,2] and Luca Ciotti[3]
[1] Institut d'Astrophysique de Paris, 98bis Bd. Arago, F-75014 Paris, France
[2] Department of Astronomy, University of Michigan, Ann Arbor, MI, USA
[3] Dipartimento di Fisica e Astronomia, Università di Bologna, via Ranzani 1, I-40127 Bologna, Italy
Received 2012 November 29; accepted 2013 March 7; published 2013 April 11

ABSTRACT

We explore how the co-evolution of massive black holes (MBHs) and galaxies is affected by environmental effects, addressing in particular MBHs hosted in the central cluster galaxies (we will refer to these galaxies in general as "CCGs"). Recently, the sample of MBHs in CCGs with dynamically measured masses has increased, and it has been suggested that these MBH masses ($M_{\rm BH}$) deviate from the expected correlations with velocity dispersion (σ) and mass of the bulge ($M_{\rm bulge}$) of the host galaxy: MBHs in CCGs appear to be "overmassive." This discrepancy is more pronounced when considering the $M_{\rm BH}$–σ relation than the $M_{\rm BH}$–$M_{\rm bulge}$ one. We show that this behavior stems from a combination of two natural factors: (1) CCGs experience more mergers involving spheroidal galaxies and their MBHs and (2) such mergers are preferentially gas poor. We use a combination of analytical and semi-analytical models to investigate the MBH–galaxy co-evolution in different environments and find that the combination of these two factors is in accordance with the trends observed in current data sets.

Key words: black hole physics – galaxies: elliptical and lenticular, cD – galaxies: evolution – galaxies: formation

Online-only material: color figures

1. INTRODUCTION

The discovery of correlations between massive black holes (MBHs) and their hosts (Magorrian et al. 1998; Ferrarese & Merritt 2000; Gebhardt et al. 2000) has been taken as one of the main elements in support of a co-evolution between MBHs and galaxies, which in turn led to the suggestion that energy input from an accreting MBH, as a quasar or active galactic nucleus (AGN), may regulate star formation in the host or create a symbiosis between MBH and stellar growth. Theoretical considerations suggest that energy- or momentum-driven outflows establish correlations that scale as $M_{\rm BH} \propto \sigma^5$ and $M_{\rm BH} \propto \sigma^4$, respectively (Silk & Rees 1998; Fabian 1999). The correlations between MBHs and galaxies, derived on a sample of about 50–70 MBHs (e.g., Gültekin et al. 2009; Graham et al. 2011; McConnell & Ma 2012), are also extrapolated to the whole population, assuming that each galaxy hosts an MBH consistent with the correlation and its scatter to derive global properties, such as the mass density in MBHs today (e.g., Shankar et al. 2004). These correlations, or deviations from such correlations, also appear to hold the key to understanding the formation and evolution of the MBH population (Volonteri 2012 and references therein).

Recent measurements of the masses of MBHs in central cluster galaxies (CCGs; we include in this definition central dominant galaxies as well as the brightest cluster galaxies) seem to suggest that these MBHs are "overmassive" compared to expectations from the $M_{\rm BH}$–σ relation, but they appear more consistent, albeit with a large scatter, with the $M_{\rm BH}$–L_V relation (McConnell et al. 2011, 2012). McConnell & Ma (2012) and Graham & Scott (2013) fit for the $M_{\rm BH}$–σ correlation finding a steep correlation, e.g., from $M_{\rm BH} \propto \sigma^{4.2}$ (Gültekin et al. 2009) to $M_{\rm BH} \propto \sigma^{5.5-5.6}$. The same does not happen for the $M_{\rm BH}$–$M_{\rm bulge}$ relation that appears to be consistent with being linear in all cases (although including MBHs in CCGs increases the normalization). There is also tentative evidence for overmassive MBHs in CCGs from comparisons with the expectations from the fundamental plane of black hole activity (Hlavacek-Larrondo et al. 2012). Feedback affecting galaxies in different ways depending on potential well (Booth & Schaye 2011; Sazonov et al. 2005) and environment, via gas-rich mergers and cooling flows (Zubovas & King 2012), has been proposed to be partially responsible for the properties of these MBHs.

We investigate here two guiding ideas related to the influence of mergers between spheroidal, gas-poor galaxies ("dry" mergers), and of MBH–MBH mergers to determine the astrophysical drivers of the possibly different relationship between MBHs and their hosts in the case of CCGs. It is well established from the theoretical point of view that (parabolic) dry mergers consistently grow a galaxy's mass, luminosity, and radius more than a galaxy's velocity dispersion (e.g., Ciotti & van Albada 2001; Nipoti et al. 2003a; Ciotti et al. 2007; Naab et al. 2009; Nipoti et al. 2009; Shankar et al. 2013; Oser et al. 2012; Hilz et al. 2013), especially when a galaxy is dominant over the general population (Ciotti et al. 2007; Naab et al. 2009). Qualitatively this implies that eventually the largest galaxies deviate from the $M_{\rm BH}$–σ relation. Therefore, if CCGs grew predominantly through dry mergers (e.g., Ostriker & Tremaine 1975; Hausman & Ostriker 1978), and their MBHs grew mostly through MBH–MBH mergers (Malbon et al. 2007; Yoo et al. 2007), then the expectation is that in such dry mergers they will be outliers in the $M_{\rm BH}$–σ relation (see also Boylan-Kolchin et al. 2006; Lauer et al. 2007; Zhang et al. 2012). Support for the influence of dry mergers in shaping the structural properties of CCGs comes from their steeper radius–luminosity relation and flatter Faber–Jackson relation (e.g., Lauer et al. 2007; Bernardi et al. 2007; Desroches et al. 2007). Additionally, if MBHs in CCGs experience a significant mass increase because of MBH–MBH mergers with respect to MBHs in a field environment, the extra boost in mass may also contribute to explain the properties of MBHs in CCGs, if gas accretion is responsible for establishing the relationships in the first place.

We present here models of MBH growth in galaxies that take into account both the cosmic environment (the frequency and properties of galaxy and MBH mergers) and the evolution of

the structural properties of galaxies during galaxy mergers, with particular attention to mergers between gas-poor spheroids.

2. BLACK HOLE GROWTH

We use the latest incarnation of our semi-analytical models (Volonteri et al. 2012) to provide a simple estimate of the influence of dry mergers on the build-up of MBHs and their hosts in different environments. We start from Monte Carlo realizations of the merger hierarchy of dark matter halos from early times to the present in a ΛCDM cosmology (WMAP5; Komatsu et al. 2009). The mass resolution is set to be 10^{-3} times the mass of the main halo at $z = 0$, and it reaches $10^5\ M_\odot$ at $z = 20$.

We summarize here the main assumptions of the semi-analytical model. We wish to keep our models as simple as possible, while making sure that the properties of the MBHs we study are correctly determined through the cosmic evolution of their hosts. We do not explicitly model in detail the complex physics of the gaseous component of galaxies through cooling, star formation, and various feedbacks (see Fanidakis et al. 2011; Fontanot et al. 2011; Hirschmann et al. 2012; Barausse 2012 and references therein for models that treat in detail semi-analytically the baryonic component of galaxies and its link to MBH evolution) even though a simple scheme taking into account gas dissipation and star formation is implemented as described in Section 3. In particular, in the present approach we follow the evolution of the three relevant cosmological components of interest, namely, (1) the dark matter halos, (2) the galaxies (stars plus gas), and (3) the central MBHs. We briefly describe how their properties are determined as a function of the merging events.

In practice, each halo is modeled as an isothermal sphere of one-dimensional velocity dispersion $\sigma_{\rm vir}$ and circular velocity $v_{\rm circ} = \sqrt{2}\sigma_{\rm vir}$. Each halo is also characterized by a virial radius r_h and a mass M_h contained within r_h, such that the mean density within the virial radius is $\Delta_{\rm vir}\,\rho_{\rm crit}$, where $\rho_{\rm crit}$ is the critical density for closure at the redshift of collapse and $\Delta_{\rm vir}$ is the density contrast at virialization for the chosen cosmology. When two halos merge, the new total mass inside the virial radius is computed as the sum of the two participating masses, and the new virial radius is determined by requiring that the mean halo density within the new r_h is $\Delta_{\rm vir}$ times the critical density at that redshift. Therefore, the new $v_{\rm circ}$ and $\sigma_{\rm vir}$ are uniquely determined. As described in the following, $\sigma_{\rm vir}$ is a fundamental ingredient in order to determine accretion on MBHs.

Galaxy morphology is related to the merger history, using a three-parameter model, where spheroid (we equivalently refer to spheroids and "gas-poor" galaxies in the following) formation depends on both the mass ratio of the two merging halos and their velocity dispersion, and the timescale over which a spheroid can re-acquire a disc through cold flows and mergers with gas-rich galaxies. Koda et al. (2009) show that the fraction of disc- versus spheroid-dominated galaxies is well explained if the only merger events that lead to spheroid formation have mass ratio >0.3 and $\sigma_{\rm vir} > 55\,{\rm km\,s^{-1}}$; also, the merger timescale (calculated following Boylan-Kolchin et al. 2008) must be less than the time between the beginning of the merger and today, $z = 0$. We assume that spheroids form after a merger that meets these requirement. In order to include the effect of gas accretion and cold flows we additionally allow gas to re-condense ("gas-rich" galaxy) after 5 Gyr in galaxies with $\sigma_{\rm vir} < 300\,{\rm km\,s^{-1}}$ where no major mergers occurred. We do not explicitly add an amount of re-accreted gas; we simply label the galaxy as "gas-rich." In Section 3, we describe in detail how "bona fide" structural galaxy properties are determined following a merger and the associated gas dissipation.

At high redshift we seed dark matter halos with MBHs created by gas collapse whose mass is linked to the halo $v_{\rm circ}$. Specifically, we adopt here the formation model detailed in Natarajan & Volonteri (2012) based on Toomre instabilities (Lodato & Natarajan 2006). The subsequent evolution of MBHs includes MBH–MBH mergers, merger-driven gas accretion, stochastic fueling of MBHs through molecular cloud (MC) capture, and a basic implementation of accretion of recycled gas from stellar evolution.

We assume that when two galaxies hosting MBHs merge, the MBHs themselves merge within the merger timescale of the host halos (Dotti et al. 2007 and references therein). We also include gravitational recoils using the formalism described in Campanelli et al. (2007). Note that in our models MBHs accrete mass whenever it is available to them. At the time of an MBH–MBH merger, we just sum the masses at that specific time. The MBHs may accrete gas driven by the galaxy merger or through accretion of MCs before the MBH–MBH merger proper, during (i.e., at the same time step) or after, i.e., on the merged MBH (as long as the MBH is not ejected from the galaxy center). Since our time steps are typically short compared to the Salpeter time ($\sim 10^5$–10^6 yr) we can keep track of accretion (including the evolution of the accretion rate) and mergers self-consistently rather than simply adding all the accreted mass at one single time step.

After a halo merger with mass ratio larger than 3:10, in which at least one of the two halos is the host of a gas-rich galaxy, we assume that a merger-driven accretion episode is triggered. The accretion rate is set at the Eddington limit until the MBH mass reaches $M_{{\rm BH},\sigma} = 5\times10^7\left(\sigma_{\rm vir}/200\,{\rm km\,s^{-1}}\right)^4\ M_\odot$. We therefore assume that it is the potential well of the host halo that sets the maximum mass at which the MBH can grow through high accretion rate accretion. After that, self-regulation ensues and the MBH feedback unbinds the gas closest to the MBH, thus reducing its feeding. We model the decrease of the accretion rate as

$$f_{\rm Edd}(t) = \left(\frac{t + t_{f_{\rm Edd}}}{t_{f_{\rm Edd}}}\right)^{-\eta_L}, \qquad (1)$$

where $\eta_L \simeq 2$ and $t_{f_{\rm Edd}} \simeq 4.1\times10^6 (M_{{\rm BH},\sigma}/10^8\ M_\odot)$ yr, and $t = 0$ (where $f_{\rm Edd} = 1$) represents the time when the MBH reaches the threshold for self-regulation (Hopkins & Hernquist 2006). Since the accretion rate $\dot M_{\rm in}(t) = f_{\rm Edd}(t)\,M_{\rm BH}(t)/t_{\rm Edd}$ is time dependent, it is integrated self-consistently at each time step to obtain the growth of the MBH mass until the accretion rate drops below $f_{\rm Edd} \simeq 10^{-5}$, at which point we consider the accretion episode concluded.

In gas-rich galaxies we include also feeding through MCs. At each time step, Δt, we determine the probability of an accretion event as

$$\mathcal{P} = \frac{\Delta t}{t_{\rm MC}} \simeq \frac{10^{-3}\sigma_{\rm vir}\Delta t}{R_{\rm cl}}, \qquad (2)$$

where $R_{\rm cl} \simeq 10$ pc (Hopkins & Hernquist 2006). We assume a lognormal distribution for the mass function of clouds close to galaxy centers (peaked at $\log(M_{\rm MC}/\ M_\odot) = 4$, with a dispersion of 0.75 based on the Milky Way case; e.g., Perets et al. 2007). In order to derive the accretion rate and duration of the accretion episode caused by the MC, we derive the properties of the accretion disc created in one of these events (including disc

Table 1
Galaxy and MBH Mergers

$M_{\rm halo}$ ($M_\odot$)	Dry Mergers with MBHs	Dry Mergers (Total)	$M_{\rm BH,0}/M_{\rm acc}$
10^{15}	3.3 ($\sigma_n = 1.8$)	3.5 ($\sigma_n = 2.1$)	10.9 ± 9.7
10^{14}	1.5 ($\sigma_n = 1.2$)	1.6 ($\sigma_n = 1.2$)	2.4 ± 1.0
4×10^{13}	0.4 ($\sigma_n = 0.6$)	0.4 ($\sigma_n = 0.6$)	1.9 ± 0.7
2×10^{13}	0.1 ($\sigma_n = 0.4$)	0.2 ($\sigma_n = 0.4$)	2.0 ± 0.7
10^{13}	0.1 ($\sigma_n = 0.3$)	0.1 ($\sigma_n = 0.3$)	1.8 ± 1.8

Notes. Number of mergers (including their 1σ variance) with mass ratio >0.1 experienced by the central galaxy, regardless of its morphology, of a halo that by $z = 0$ has the mass listed in Column 1, and growth channels for its MBH.

size, R_d, mass, M_d, accretion rate, and duration of the accretion episode). We assume that the MBH captures only material passing within the Bondi radius, R_B, and that its specific angular momentum is conserved (Bottema & Sanders 1986; Wardle & Yusef-Zadeh 2008). The outer edge of the disc that forms around the MBH corresponds to the material originally at R_B:

$$R_d = 2\lambda^2 R_B = 8.9\,{\rm pc}\,\lambda^2 \frac{M_{\rm BH}}{10^7\,M_\odot}\left(\frac{\sigma_{\rm vir}}{100\,{\rm km\,s^{-1}}}\right)^{-2}, \quad (3)$$

where λ is the fraction of angular momentum retained by gas during circularization. The maximum captured mass will be contained in a cylinder with a radius R_B and length $2 \times R_{\rm cl}$, the MC diameter. If κ is the ratio of the mass going into the disc with respect to the whole mass in the cylinder, then

$$M_d = \kappa \frac{R_B}{R_{\rm cl}} M_{\rm MC} = 4.7 \times 10^4 \kappa \left(\frac{M_{\rm BH}}{10^7\,M_\odot}\right)^2 \left(\frac{\sigma_{\rm vir}}{100\,{\rm km\,s^{-1}}}\right)^{-4} M_\odot. \quad (4)$$

We assume that the disc is consumed over its viscous timescale

$$t_{\rm visc} = \left(\frac{R_d^3}{\alpha_v^2 G M_d}\right)^{1/2} = 3.4 \times 10^5 \frac{\lambda^3}{\alpha_v} \frac{M_{\rm BH}}{10^7\,M_\odot}\left(\frac{\sigma_{\rm vir}}{100\,{\rm km\,s^{-1}}}\right)^{-3} {\rm yr}, \quad (5)$$

so that we can calculate an upper limit to the mean accretion rate

$$\dot{M}_{\rm max} = \frac{M_d}{t_{\rm visc}} = 0.13 \frac{\alpha_v \kappa}{\lambda^3} \frac{M_{\rm BH}}{10^7\,M_\odot}\left(\frac{\sigma_{\rm vir}}{100\,{\rm km\,s^{-1}}}\right)^{-1} N_{23}\,M_\odot\,{\rm yr}^{-1}, \quad (6)$$

where N_{23} is the column density in the cloud in units of 10^{23} cm^{-2}, and $\alpha_v = 0.1$ is the viscosity parameter. Following Wardle & Yusef-Zadeh (2012) we set $\lambda = 0.3$ and $\kappa = 1$. If $\dot{M}_{\rm max}$ is less than the Eddington rate (assuming a radiative efficiency of 10%) we let the MBH accrete the whole M_d over a time $t_{\rm visc}$, otherwise we treat accretion in a way similar to the "decline" phase of quasars, as feedback from the high luminosity produced by accreting the cloud will limit the amount of material the MBH can effectively swallow.

In gas-poor galaxies, feeding of an MBH can be sustained by the recycled gas (primarily from red giant winds and planetary nebulae) of the evolving stellar population (e.g., Ciotti & Ostriker 1997; Novak et al. 2012). The geometrical model by Volonteri et al. (2011) implies that the quiescent level of accretion onto a central MBH due to recycled gas is $f_{\rm Edd} \simeq 10^{-5}$.

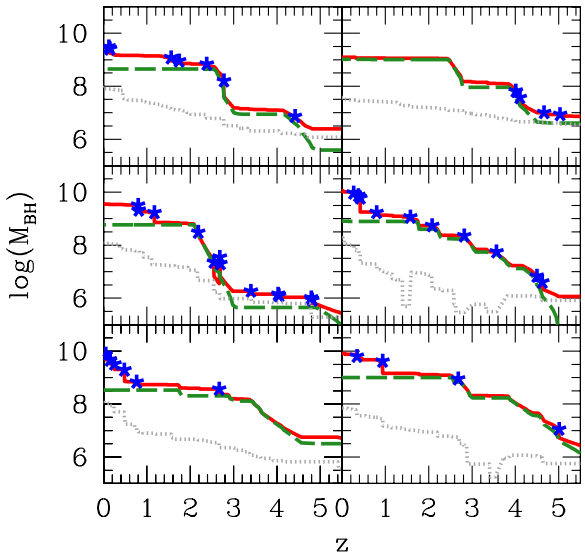

Figure 1. Examples of MBH growth in six randomly chosen central galaxies of $10^{15}\,M_\odot$ halos. The red solid curve shows the MBH mass at a given time, the dark green dashed curve shows the cumulative mass gained in accretion events, and blue asterisks mark MBH–MBH mergers with mass ratio >1:10. The dotted gray curve shows the curves we obtained for the same MBHs when we "turned-off" all accretion channels, so that the only growth mechanism is through MBH–MBH mergers (the decrease in MBH masses in such curves are due to dynamical ejections of MBH, not to evaporation or mass loss). As an example, the growth of the MBH in the top-left panel is dominated by MBH–MBH mergers, while that of the MBH in the top-right panel is dominated by accretion through various channels (merger driven in gas-rich mergers, through accretion of gas clouds, and through recycled gas).

(A color version of this figure is available in the online journal.)

Through this model we can disentangle what the main contributions to the growth of MBHs and galaxies in different halos are. As regards galaxies, in Table 1 we list the number of dry mergers experienced over its lifetime by the central galaxy of a halo, as a function of the halo mass at $z = 0$ (the average is performed over 20–35 different halos for each halo mass). We can consider the $10^{15}\,M_\odot$ halo as a cluster-sized halo, the $10^{14}\,M_\odot$ halo as a group-sized halo, and the smaller halos as galaxy-sized ones. The dryness of a galaxy during a merger is determined in a very simple way, i.e., we require that both merging galaxies are gas poor. As a reference the total number of mergers (dry and wet) with mass ratio >0.1 experienced by the same galaxies since $z = 4$ is typically between 8 and 12. As expected, the number of dry mergers decreases as the halo mass decreases; therefore, their influence will be strongest for central galaxies in clusters and possibly in groups. As highlighted in Column 2, most, but not all, dry mergers involve galaxies hosting MBHs.

In Figure 1, we focus on the MBH growth in six different realizations of $10^{15}\,M_\odot$ halos. For instance, the growth of the two MBHs in the top panels is strikingly different. In one case it is dominated by MBH–MBH mergers at $z < 2$, while in the second case MBH does not experience any important MBH–MBH merger at late cosmic time. If we define the relative growth through mergers as the difference between the MBH mass at $z = 0$, $M_{\rm BH,0}$, and the cumulative accreted gas mass,

$M_{\rm acc}$, i.e., we sum all the gas mass that is added to this MBH in all accretion episodes throughout its lifetime, we can estimate the importance of MBH–MBH mergers in an MBH's history. In Table 1 we report this information in the fourth column. Note that the definition we adopt does *not* account for gas accretion on the MBHs that merge with the one in the central galaxy. Therefore, the fact that in general $M_{\rm BH,0}/M_{\rm acc} > 1$ does *not* mean that MBHs grow predominantly through mergers, and in fact if we ignored all accretion onto MBHs from our models, the final MBH mass would be about two orders of magnitude smaller (cf. gray dotted curves in Figure 1). Overall, therefore, MBHs grow through accretion of gas in a way consistent with independent estimates (Yu & Tremaine 2002).

To test the robustness of our results, we changed the MBH feeding scheme by assuming that all MBH accretion activity is driven by galaxy mergers, that the accretion rate is fixed to 30% of the Eddington rate, and that accretion stops once the MBHs have reached the value of $M_{\rm BH,\sigma}$. We find that while small quantitative differences exist, qualitatively the results of our investigation are unchanged. We conclude that if the $M_{\rm BH}$–σ relation is established because of accretion-driven feedback (e.g., Silk & Rees 1998; Fabian 1999), MBHs in CCGs may not necessarily obey the same $M_{\rm BH}$–σ relation, as their masses may grow substantially through mergers after accretion dwindles.

3. MERGERS AND GALAXY STRUCTURE

From the evolutionary histories of our models we extract the series of mergers that the central galaxy of the main halo experiences from $z = 1$. We record the MBH mass in the merging galaxies and the dark matter halo masses within the virial radius, M_{h1} and M_{h2}, (hereafter the subscripts refer to each one of the two galaxies with the convention that subscript 1 labels the central galaxy of the main halo, which is not necessarily the most massive galaxy of the merging pair). To each halo at the starting redshift, we assign a stellar mass, M_*, using the fits by Behroozi et al. (2010; see also Nipoti et al. 2012). If a galaxy is identified as gas-rich, we assume that only 75% of the stars are distributed in the spheroidal part. We then assign a mass-to-light ratio, a projected velocity dispersion, σ, consistent with the Faber–Jackson relation, and an effective radius determined through the fundamental plane (Binney & Tremaine 2008, p. 23–24) including scatter in all relations. We included a redshift dependence of the Faber–Jackson and Kormendy relations, using the scalings suggested by Oser et al. (2012), namely that $\sigma \propto (1+z)^{0.44}$ and $R_{\rm e} \propto (1+z)^{-1.44}$ (see also Nipoti et al. 2012). We then calculate M_*, R_e, and σ resulting from the merger as follows (Ciotti et al. 2007). We account for weak homology by relating σ to the galaxy virial velocity dispersion, σ_v, and R_e to the galaxy virial radius, r_v, as

$$\frac{\sigma}{\sigma_v} \simeq \frac{24.31 + 1.91n + n^2}{44.23 + 0.025n + 0.99n^2}, \quad (7)$$

$$\frac{r_v}{R_{\rm e}} \simeq \frac{250.26 + 7.15n}{77.73 + n^2}, \quad (8)$$

adequate for Sérsic index n, $2 \lesssim n \lesssim 12$. We assume that the Sérsic index of the resulting galaxy is $n = 1 + \max(n_1, n_2)$, where n_1 and n_2 are the Sérsic indices of the progenitors (each galaxy starts with n determined inverting the virial identity $GM_*/R_{\rm e}\sigma^2 = (r_v/R_{\rm e}) \times (\sigma_v/\sigma)^2$ for given σ and $R_{\rm e}$).

In the case of mergers between gas-rich galaxies or between a gas-poor and a gas-rich galaxy, we assume that each gas-rich galaxy has a gas mass $M_g = \alpha M_*$, with $\alpha = 4$ for all galaxies independently of their histories and that a fraction $\eta = 0.05\,(M_{h2}/M_{h1})$ of the gas is converted into stars:

$$M_* = M_{*1} + M_{*2} + \eta(M_{g1} + M_{g2}). \quad (9)$$

We find the velocity dispersion of the newly formed galaxy[4] as

$$\sigma_v^2 = \frac{M_{\rm gal1}}{M_{\rm gal}} A_1 \sigma_{v1}^2 + \frac{M_{\rm gal2}}{M_{\rm gal}} A_2 \sigma_{v2}^2, \quad (10)$$

where $M_{\rm gal1} = M_{*1} + M_{g1}$, $M_{\rm gal2} = M_{*2} + M_{g2}$, $M_{\rm gal} = M_{\rm gal1} + M_{\rm gal2}$, and

$$A_1 = 1 + \frac{\eta\alpha_1}{1+\alpha_1}, \quad (11)$$

and a similar expression holds for A_2. From the second merger of the sequence onward, the central galaxy retains the properties derived in the previous step, while we assign M_{*2} and σ_{v2} to the merging galaxy as described above. Throughout our experiment, the MBH mass is determined from the semi-analytical model that includes both accretion and MBH–MBH mergers. We note that not all galaxies host MBHs, i.e., the merging galaxy may or may not contribute to the MBH growth.

We present the results of this experiment in Figures 2 and 3. In Figure 2, we compare the velocity dispersion distribution function of modeled galaxies to distribution functions at $z = 0$ and $z = 1$ (Sheth et al. 2003; Bezanson et al. 2011), showing an adequate agreement, except for an underestimate of galaxies with very high σ at $z = 1$. In the top two panels of Figure 3, we

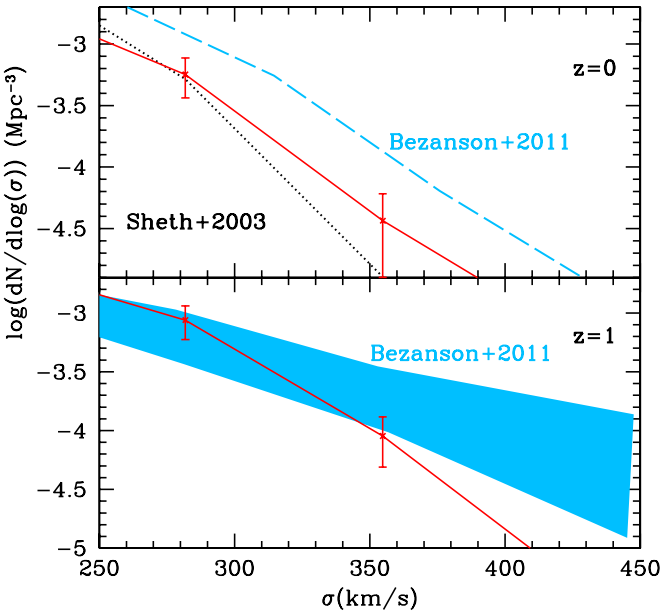

Figure 2. Velocity dispersion distribution functions at $z = 0$ (top) and $z = 1$ (bottom). The model (red solid curve) is compared to distribution functions derived from different surveys (at $z = 0$ we show the function derived by Sheth et al. (2003), as well as the correction introduced by Bezanson et al. (2011) to account for scatter). At $z = 1$ we report the range of values from Figure 3 in Bezanson et al. (2011).

(A color version of this figure is available in the online journal.)

[4] The presence of dark matter can be included through an extra $\alpha_{\rm DM}$ parameter in our scheme (see Ciotti et al. 2007), assuming that stars and dark matter are similarly distributed. Inclusion of the dark matter halo represents a small correction as long as we are interested in the region within the effective radius.

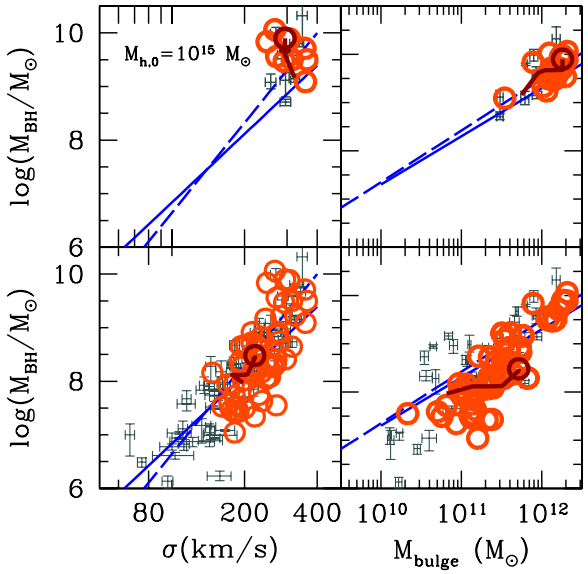

Figure 3. Examples of $M_{\rm BH}$–σ and $M_{\rm BH}$–$M_{\rm bulge}$ in 20 randomly chosen central galaxies of $10^{15}\,M_\odot$ (top) and 10^{13}–$10^{15}\,M_\odot$ (bottom) halos. The gray error bars are observed MBHs and galaxies (McConnell & Ma 2012; in the top panel we show CCGs only), the solid blue lines are the fits derived by Gültekin et al. (2009) and Marconi & Hunt (2003), and the dashed lines are the fits from McConnell & Ma (2012). The red dots show the location of model MBHs at $z = 0$. The dark red curves show two examples from the evolutionary histories: horizontal rightward swings in the $M_{\rm BH}$–σ plots occur when the galaxy merges with a more massive galaxy and vertical (leftward) movement is characteristic of dry mergers with similar (smaller) galaxies.

(A color version of this figure is available in the online journal.)

focus on MBHs hosted in the central galaxy of $10^{15}\,M_\odot$ halos at $z = 0$ (akin to CCGs), while in the bottom panel we include all MBHs in halos with mass $>10^{13}\,M_\odot$ at $z = 0$. At lower masses secular processes are likely to dominate over mergers and our model is less suitable to describe their evolution. We assessed that the results at $z = 0$ are qualitatively unchanged if we ignore the redshift evolution in the Faber–Jackson and Kormendy relations, with MBHs and galaxies occupying the same region in the $M_{\rm BH}$–σ relation. CCGs are characterized by MBHs that consistently deviate from the expected correlations, being overmassive at fixed galaxy properties, occupying the same range as observations. MBHs in elliptical galaxies that are not CCGs, where the influence of MBH–MBH mergers and dry mergers is much milder, tend instead to sit closer to the global MBH–host correlations. This result can be interpreted as overall steeper and higher normalized relations with respect to previous estimates (compare solid and dashed black lines in Figure 2). At $z < 1$ most CCGs are the dominant galaxies, and they merge with smaller galaxies that consistently have $\sigma_{v2} < \sigma_{v1}$ and therefore their velocity dispersion cannot increase (see Equation (10)). On the other hand, a non-CCG galaxy has a higher chance of merging with a galaxy with $\sigma_{v2} > \sigma_{v1}$, with the merger remnant having $\sigma_v > \sigma_{v1}$ (see the dark red tracks in Figure 2 for an example).

We note (see also Nipoti et al. 2012) that this scheme tends to overproduce stellar masses by $z = 0$. In fact the $M_{\rm star}$–$M_{\rm h}$ relationship peaks at $M_{\rm h} = 10^{12}\,M_\odot$; therefore, by merging galaxies close to the peak the remnant galaxy ends up having an increased $M_{\rm star}$–$M_{\rm h}$. While our merger sequence includes both galaxies below, at, and above the peak, we find that we consistently overpredict stellar masses at $z = 0$ with respect to the scaling we would obtain directly from the $M_{\rm star}$–$M_{\rm h}$ relationship, and that in general bulges appear too massive (this is evident in the bottom-right panel of Figure 3). This problem would be alleviated if we included corrections for mass lost in the merging process (Nipoti et al. 2003a). We also consider parabolic mergers only, where energy is perfectly conserved. However, not all mergers involving a CCG are necessarily parabolic. On the one hand, since the galaxies move in the potential of the cluster, hyperbolic mergers may occur. On the other hand, Nipoti et al. (2003b) note the effect of dynamical friction that braking the galaxy's orbit may induce elliptical merging. Hyperbolic and negative-energy mergers involving a bound pair have competitive effects on the evolution of σ. Mergers with negative orbital energy increase the final σ and vice versa. Hilz et al. (2013) also suggest that energy transfer from bulge to halo grows the velocity dispersion further.

4. CONCLUSIONS

In this paper we have highlighted the effects that mergers have on the MBH population in CCGs. Two main factors contribute to their evolution. First, CCGs experience many more dry mergers with spheroids than other galaxies. Parabolic dry mergers grow a galaxy's mass, luminosity, and radius more than a galaxy velocity dispersion (e.g., Ciotti & van Albada 2001; Nipoti et al. 2003a; Ciotti et al. 2007; Naab et al. 2009; Nipoti et al. 2009; Shankar et al. 2013; Oser et al. 2012; Hilz et al. 2013). If in a given merger $M_{\rm BH}$ and $M_{\rm bulge}$ increase relatively more than σ (see the discussion in Ciotti et al. 2007; Ciotti 2009), a sequence of such mergers will lead to more massive MBHs at fixed σ. In Figure 2 (left panels), this corresponds to moving upward more efficiently than rightward.

Second, the sheer number and mass contribution of MBH–MBH mergers occurring in CCGs galaxies are much higher than in other galaxies (see Table 1). If correlations between MBHs and hosts were established through quasar/AGN feedback (e.g., Silk & Rees 1998; Fabian 1999; Di Matteo et al. 2005; Hopkins et al. 2009), and MBH mergers contribute to the MBH growth *after* the bulk of quasar/AGN activity has ceased (Figure 1), then the MBH mass increase brought by these mergers will then push the MBH upward and out from the $M_{\rm BH}$–σ correlation established through feedback. One important caveat, however, is whether MBH binaries can merge efficiently in gas-poor environments, because of the so-called final parsec problem (e.g., Begelman et al. 1980), although various effects, such as triaxiality and rotation, as well as the presence of massive perturbers, may increase the orbital decay rate (see Colpi & Dotti 2011 for a recent review). The presence of multiple MBHs may also occur (Haehnelt & Kauffmann 2002; Volonteri et al. 2003; Kulkarni & Loeb 2012).

Our models are at variance with other models that study the impact of MBH mergers on the establishment of correlations (e.g., Jahnke & Macciò 2011) as we do not assume that MBHs populate all galaxies. In fact, the presence or absence of a central MBH leads to different evolutionary paths in the $M_{\rm BH}$–σ and $M_{\rm BH}$–$M_{\rm bulge}$ relations. We can consider two extreme cases. Let us assume that all galaxies host an MBH. Then at each merger M_* and $M_{\rm BH}$ increase as the sum of those in the two galaxies, barring for the effects of stellar escapers (Nipoti et al. 2003a; Hilz et al. 2013) and nonlinear addition of MBH masses (Ciotti & van Albada 2001; Ciotti et al. 2007). However, Equation (3) shows that σ would stay the same or slightly decrease. This corresponds to a vertical upward movement in the $M_{\rm BH}$–σ plot, eventually leading to MBHs that are overmassive for their σ, but are not outliers in the $M_{\rm BH}$–$M_{\rm bulge}$ correlation. The other

extreme case assumes that only the main galaxy hosts an MBH. Then at each merger M_* increases, while $M_{\rm BH}$ and σ do not. Eventually, the MBH in the galaxy that results from the merger sequence will be undermassive for its bulge mass, but it will not be an outlier in the $M_{\rm BH}$–σ relation.

Broadly speaking, the models of MBH evolution that we adopt for this paper (Volonteri et al. 2012) predict that the most massive MBHs, except for those hosted in CCGs, are those that are best correlated with their hosts (Volonteri & Natarajan 2009) if their build-up is driven by a combination of accretion and mergers that includes both gas-rich and gas-poor galaxies, and dispersion should increase at low MBH/galaxy masses (see Figure 2, top panel in Volonteri et al. 2012), where the MBH mass, even at $z = 0$, traces the properties of the MBH formation mechanism (van Wassenhove et al. 2010). It may well be that if different processes shape the MBH mass at different galaxy masses (MBH formation at the lowest masses, AGN feedback at intermediate masses, MBH and dry mergers at the highest masses), there is not a unique link that straddles throughout the whole range.

We are warmly grateful to C. Nipoti and K. Gültekin for insightful comments. M.V. acknowledges funding support from NASA, through Award Number ATP NNX10AC84G; from SAO, through Award Number TM1-12007X; from NSF, through Award Number AST 1107675; and from a Marie Curie Career Integration grant (PCIG10-GA-2011-303609). L.C. acknowledges financial support from PRIN MIUR 2010-2011 project "The Chemical and Dynamical Evolution of the Milky Way and Local Group Galaxies," prot. 2010LY5N2T.

REFERENCES

Barausse, E. 2012, MNRAS, 423, 2533
Begelman, M. C., Blandford, R. D., & Rees, M. J. 1980, Natur, 287, 307
Behroozi, P. S., Conroy, C., & Wechsler, R. H. 2010, ApJ, 717, 379
Bernardi, M., Hyde, J. B., Sheth, R. K., Miller, C. J., & Nichol, R. C. 2007, AJ, 133, 1741
Bezanson, R., van Dokkum, P. G., Franx, M., et al. 2011, ApJL, 737, L31
Binney, J., & Tremaine, S. 2008, Galactic Dynamics (2nd ed.; Princeton, NJ: Princeton Univ. Press)
Booth, C. M., & Schaye, J. 2011, MNRAS, 413, 1158
Bottema, R., & Sanders, R. H. 1986, A&A, 158, 297
Boylan-Kolchin, M., Ma, C.-P., & Quataert, E. 2006, MNRAS, 369, 1081
Boylan-Kolchin, M., Ma, C.-P., & Quataert, E. 2008, MNRAS, 383, 93
Campanelli, M., Lousto, C. O., Zlochower, Y., & Merritt, D. 2007, PhRvL, 98, 231102
Ciotti, L. 2009, NCimR, 32, 1
Ciotti, L., Lanzoni, B., & Volonteri, M. 2007, ApJ, 658, 65
Ciotti, L., & Ostriker, J. P. 1997, ApJL, 487, L105
Ciotti, L., & van Albada, T. S. 2001, ApJL, 552, L13
Colpi, M., & Dotti, M. 2011, ASL, 4, 181
Desroches, L.-B., Quataert, E., Ma, C.-P., & West, A. A. 2007, MNRAS, 377, 402
Di Matteo, T., Springel, V., & Hernquist, L. 2005, Natur, 433, 604
Dotti, M., Colpi, M., Haardt, F., & Mayer, L. 2007, MNRAS, 379, 956
Fabian, A. C. 1999, MNRAS, 308, L39
Fanidakis, N., Baugh, C. M., Benson, A. J., et al. 2011, MNRAS, 410, 53
Ferrarese, L., & Merritt, D. 2000, ApJ, 539, L9
Fontanot, F., Pasquali, A., De Lucia, G., et al. 2011, MNRAS, 413, 957
Gebhardt, K., Bender, R., Bower, G., et al. 2000, ApJ, 539, L13
Graham, A. W., Onken, C. A., Athanassoula, E., & Combes, F. 2011, MNRAS, 412, 2211
Graham, A. W., & Scott, N. 2013, ApJ, 764, 151
Gültekin, K., Richstone, D. O., Gebhardt, K., et al. 2009, ApJ, 698, 198
Haehnelt, M. G., & Kauffmann, G. 2002, MNRAS, 336, L61
Hausman, M. A., & Ostriker, J. P. 1978, ApJ, 224, 320
Hilz, M., Naab, T., Ostriker, J. P., et al. 2013, MNRAS, 429, 2924
Hirschmann, M., Somerville, R. S., Naab, T., & Burkert, A. 2012, MNRAS, 426, 237
Hlavacek-Larrondo, J., Fabian, A. C., Edge, A. C., & Hogan, M. T. 2012, MNRAS, 424, 224
Hopkins, P. F., & Hernquist, L. 2006, ApJS, 166, 1
Hopkins, P. F., Murray, N., & Thompson, T. A. 2009, MNRAS, 398, 303
Jahnke, K., & Macciò, A. V. 2011, ApJ, 734, 92
Koda, J., Milosavljević, M., & Shapiro, P. R. 2009, ApJ, 696, 254
Komatsu, E., Dunkley, J., Nolta, M. R., et al. 2009, ApJS, 180, 330
Kulkarni, G., & Loeb, A. 2012, MNRAS, 422, 1306
Lauer, T. R., Faber, S. M., Richstone, D., et al. 2007, ApJ, 662, 808
Lodato, G., & Natarajan, P. 2006, MNRAS, 371, 1813
Magorrian, J., Tremaine, S., Richstone, D., et al. 1998, AJ, 115, 2285
Malbon, R. K., Baugh, C. M., Frenk, C. S., & Lacey, C. G. 2007, MNRAS, 382, 1394
Marconi, A., & Hunt, L. K. 2003, ApJL, 589, L21
McConnell, N. J., & Ma, C.-P. 2012, arXiv:1211.2816
McConnell, N. J., Ma, C.-P., Gebhardt, K., et al. 2011, Natur, 480, 215
McConnell, N. J., Ma, C.-P., Murphy, J. D., et al. 2012, ApJ, 756, 179
Naab, T., Johansson, P. H., & Ostriker, J. P. 2009, ApJL, 699, L178
Natarajan, P., & Volonteri, M. 2012, MNRAS, 422, 2051
Nipoti, C., Londrillo, P., & Ciotti, L. 2003a, MNRAS, 342, 501
Nipoti, C., Stiavelli, M., Ciotti, L., Treu, T., & Rosati, P. 2003b, MNRAS, 344, 748
Nipoti, C., Treu, T., & Bolton, A. S. 2009, ApJ, 703, 1531
Nipoti, C., Treu, T., Leauthaud, A., et al. 2012, MNRAS, 422, 1714
Novak, G. S., Ostriker, J. P., & Ciotti, L. 2012, MNRAS, 427, 2734
Oser, L., Naab, T., Ostriker, J. P., & Johansson, P. H. 2012, ApJ, 744, 63
Ostriker, J. P., & Tremaine, S. D. 1975, ApJL, 202, L113
Perets, H. B., Hopman, C., & Alexander, T. 2007, ApJ, 656, 709
Sazonov, S. Y., Ostriker, J. P., Ciotti, L., & Sunyaev, R. A. 2005, MNRAS, 358, 168
Shankar, F., Marulli, F., Bernardi, M., et al. 2013, MNRAS, 428, 109
Shankar, F., Salucci, P., Granato, G. L., De Zotti, G., & Danese, L. 2004, MNRAS, 354, 1020
Sheth, R. K., Bernardi, M., Schechter, P. L., et al. 2003, ApJ, 594, 225
Silk, J., & Rees, M. J. 1998, A&A, 331, L1
van Wassenhove, S., Volonteri, M., Walker, M. G., & Gair, J. R. 2010, MNRAS, 408, 1139
Volonteri, M. 2012, Sci, 337, 544
Volonteri, M., Dotti, M., Campbell, D., & Mateo, M. 2011, ApJ, 730, 145
Volonteri, M., Madau, P., & Haardt, F. 2003, ApJ, 593, 661
Volonteri, M., & Natarajan, P. 2009, MNRAS, 400, 1911
Volonteri, M., Sikora, M., Lasota, J.-P., & Merloni, A. 2012, arXiv:1210.1025
Wardle, M., & Yusef-Zadeh, F. 2008, ApJL, 683, L37
Wardle, M., & Yusef-Zadeh, F. 2012, ApJL, 750, L38
Yoo, J., Miralda-Escudé, J., Weinberg, D. H., Zheng, Z., & Morgan, C. W. 2007, ApJ, 667, 813
Yu, Q., & Tremaine, S. 2002, MNRAS, 335, 965
Zhang, X., Lu, Y., & Yu, Q. 2012, ApJ, 761, 5
Zubovas, K., & King, A. R. 2012, MNRAS, 426, 2751